R. & M. No. 1945
(5258 & 5394)
A.R.C. Technical Report

MINISTRY OF AIRCRAFT PRODUCTION

AERONAUTICAL RESEARCH COMMITTEE
REPORTS AND MEMORANDA

Derivative Measurements and Flutter Tests on a Model Tapered Wing

By

W. P. JONES, M.A., and N. C. LAMBOURNE, B.Sc.,
of the Aerodynamics Division, N.P.L.

LONDON : HIS MAJESTY'S STATIONERY OFFICE
Price 3*s.* 0*d.* net

Derivative Measurements and Flutter Tests on a Model Tapered Wing

By

W. P. JONES, M.A., and N. C. LAMBOURNE, B.Sc.,
OF THE AERODYNAMICS DIVISION, N.P.L.

Reports and Memoranda No. 1945

6th August, 1941

§1. *Introduction and Summary.*—The influence of various parameters, such as wing density and flexural stiffness on the critical speed of a tapered wing was investigated theoretically in R. & M. 1782[1] using certain fundamental aerodynamic derivative coefficients. The principal object of the present wind-tunnel tests was to provide an experimental confirmation of the theory. A semi-rigid model wing of the R. & M. 1782[1] type was constructed with two tapered wooden spars of cruciform cross section. Its flexural axis lay at 0·3 chord and its inertia axis at 0·4 chord behind the leading edge.

Measurements were made by the forced oscillation method of the following aerodynamical derivatives for a range of values of the frequency parameter λ_0 ($\equiv 2\pi fc_0/V$):

(i) Flexural Damping,
(ii) Torsional Damping,
(iii) Torsional Stiffness.

The still air torsional damping which included the damping due to the internal structure of the wing was also measured, and the virtual inertia* effects due to the external air were estimated by two-dimensional strip theory as described in Ref. 3.

Preliminary measurements of derivatives by the forced oscillation method indicated that, for amplitudes $\theta_1 < 2{\cdot}5$ degrees of the forced motion in twist, the torsional damping and stiffness derivatives as well as the still air resonance frequency increased with decreasing amplitude. This was probably due to the variation in internal friction with amplitude. In order to avoid these effects, the experimental range of forced amplitudes was limited to $2{\cdot}5$ degrees $< \theta_1 < 5{\cdot}0$ degrees. Hence the values of the torsional derivatives given in this note would correspond to maintained flutter oscillations within this amplitude range (see Figs. 9, 10, 11, and Table 1).

The divergence speed of the wing corresponding to an elastic torsional stiffness $m_0 = 2{\cdot}87$ lb.ft./rad. was investigated in some detail. The static torsional stiffness derivative was also measured, and the critical divergence speeds deduced from the value obtained were in good agreement with the experimental results for various wing stiffnesses (see Tables 2*a* and 2*b*).

In the flutter tests the wing masses were varied to give two inertial conditions (Nos. I and II), and the procedure in these tests was to keep the torsional stiffness constant at (i) $m_0 = 2{\cdot}52$

* Referred to as aerodynamic inertia in some reports.

and (ii) $m_0 = 10{\cdot}45$ and vary the flexural stiffness so that the stiffness ratio parameter $r \left(\equiv \frac{l_\phi}{d^3} \Big/ \frac{m_0}{dc_m^{-2}} \right)$ covered the range $0 < r < 17{\cdot}5$. Three critical speeds were observed corresponding to :

(i) Spontaneous flutter,
(ii) Flutter induced by an initial twist of 2·5 degrees,
(iii) Maintained oscillations of 2·5 degrees amplitude artificially initiated.

The frequencies of the maintained oscillations were also measured for various values of r. All the experimental results are plotted against r in Figs. 13, 14 and 15 and compared with the corresponding theoretical values obtained by using various sets of derivatives (see §9).

The effect of wing tip shape on flutter was also investigated.

§2. *Description of Wing.*—A diagram and a photograph of the wing showing its internal construction are given in Figs. 1a and 1b. The chordwise wing-section was N.A.C.A.23012 with a thickness-chord ratio of 0·12.[7] The spars, which were of cruciform cross-section and very stiff in flexure, carried light ribs connected at the leading and trailing edges by thin wooden splines. Silk, doped with a solution of vaseline and chloroform, was used as covering. The spars were independently hinged at the root to a turn-table fixed to the wall of the wind-tunnel, and the wing was supported horizontally by external helical springs, which provided the flexural stiffness of the system (see Fig. 2). These springs were attached above and below the wing to a special ball-joint fitting mounted at 0·3c from the leading edge in the reference section, which lay at 0·7s from the wing root (see Figs. 1a, 1b, and 5). As the wing had no inherent flexural stiffness, the flexural axis position was determined by the point of attachment of the springs. Since the spars were very stiff in flexure and freely hinged at the root, the flexural mode of deformation was effectively linear. The torsional mode depended almost entirely on the differential displacement of the spars (see Figs. 6 and 7).

The mass of the wing was varied by clamping weights to the spars at certain positions M_1, M_1', etc., where the cover could conveniently be removed (see Fig. 1a). In all cases the axis of inertia was maintained at 0·4 chord, and the wing density per unit span was made roughly proportional to c^2. Any twist due to gravity or aerodynamic load was corrected by means of a helical spring cross-connecting the spars at the root (see Fig. 1b). This spring could be twisted to give the desired amount of correcting torque by means of a ratchet and clutch device which was operated from outside the wind tunnel.

The principal dimensions were :—

Span $s = 54$ in., reference section at $l = 0{\cdot}7s$, $d = 0{\cdot}9s$,
root chord $c_0 = 24{\cdot}3$ in., mean chord $c_m = 0{\cdot}762c_0$, tip chord $c_t = 12{\cdot}7$ in.

The inertial constants determined experimentally by resonance tests in still air are given in Table 3. The allowances for virtual inertia effects, estimated as in Ref. 4, are also tabulated.

§3. *Measurement of Modes.*—The reference axes 0 (X, Y, Z) are as shown in Fig. 5. The displacement z at any point is given by

$$z = \phi l f(\eta) + \theta x F(\eta), \qquad (1)$$

where ϕl is the flexural displacement at the reference section and θ is the twist relative to the root chord.

The functions $f(\eta)$, $F(\eta)$ define the flexural and torsional modes respectively, and were measured by the following method.

A number of spark-gaps were fitted in series along the leading and trailing edges of the wing and connected to the secondary terminals of an induction coil. The primary circuit of the coil was interrupted by means of a valve-driven tuning fork which vibrated at 50 cycles per second and produced a spark for each cycle. The sparks were photographed by two moving film cameras, and all the information required regarding the motion or deformation of the wing was obtained from the records. The depth of focus of each camera was increased by turning the lens through a small angle relative to the centre line of the film so that the sparks could be photographed at an angle from a position close to the wing tip. A typical spark record of the motion of the trailing edge is shown in Fig. 3. The spots at the bottom of the record correspond to the spark-gap fitted at the wing root, and these are spaced at equal intervals when the film speed is constant; those at the top represent the motion at the wing tip. The displacements of all the spots in a particular column from their respective mean positions were measured by means of a projector, and by consideration of the displacements for a number of columns, the motion of the wing was determined with reasonable accuracy.

This method is very convenient for measuring static and oscillatory modes in still air as the wing can then be mounted outside the wind-tunnel and the sparks photographed directly. A record of the motion of the wing while fluttering in the wind-tunnel could have been obtained by photographing the images of the spark-gaps in suitably placed mirrors near the wing tip with two cameras mounted on the wind-tunnel roof, but it was assumed in the present tests that the flutter modes were sensibly independent of wind speed over the speed range of the experiments.

§4. *Aerodynamic Flexural Damping.*—The flexural damping was measured by the forced oscillation method. The wing was constrained to move in flexure only by means of two bridles of wires attached to the wing at the reference section. The forced and forcing motions were recorded photographically on moving film by means of two pea lamps, which were carried on two freely hinged rocker arms mounted on the wind-tunnel roof and operated by the forcing drive and by the wing respectively. A time scale was provided by a single spark-gap which produced fifty sparks a second (see §3). From a knowledge of the amplitudes of the forced and forcing motions and the phase difference, the flexural damping was determined.

A few measurements were also made by the method of free decaying oscillations. The flexural damping was in this case estimated from the rate of decay and the frequency of the motion; the effective flexural moment of inertia being known.

The results obtained by the different methods were in good agreement and are plotted against λ_0 ($\equiv 2\pi fc_0/V$) in Fig. 9. Theoretical values deduced from Refs. 1 and 2 are included for comparison.

§5. *Aerodynamic Torsional Derivatives.*—In this case, the wires attached to the reference centre of the wing were firmly held, and the wing was forced in twist through a spring connected to the leading edge of the reference section. A further spring was attached to the same point and earthed to the tunnel floor in order to maintain tension in the forcing wire. The forced and forcing motions were recorded by means of the rocker arm system referred to in §4. A typical record is shown in Fig. 4.

In the usual notation, the equation of motion for a forced oscillation of this type in an airstream is of the form

$$(G_3 - M_{\ddot{\theta}})\,\ddot{\theta} - M_{\dot{\theta}}\dot{\theta} + (m_\theta - M_\theta)\,\theta = \theta_0 \sin pt, \qquad (2)$$

where G_3 here denotes the total effective inertia of the system and m_θ is the torsional stiffness. The solution of (2) can be expressed as

$$\theta = \theta_1 \sin (pt + \varepsilon),$$

where

$$-M_{\dot{\theta}}p = (\theta_0/\theta_1) \sin \varepsilon \qquad (3)$$

and

$$S(V, p) \equiv m_\theta - M_\theta - (G_3 - M_{\ddot{\theta}})\,p^2 = (\theta_0/\theta_1) \cos \varepsilon \qquad (4)$$

For $V = 0$, it is assumed that $M_\theta = 0$, and that $- M_{\ddot{\theta}} = I_E$ the virtual inertia of the wing due to the external air. The still air torsional damping includes any structural damping that may be present.

Forced oscillation tests were made for various wind speeds and frequencies, and the values of θ_0, θ_1, p and ε were determined by analysis of the photographic records.

For the wing tested, the torsional derivatives increased with decreasing amplitude and were only constant for $\theta_1 > 2{\cdot}5$ degrees for a particular frequency. It was also noted that the resonance frequency in still air increased with decreasing amplitude for $\theta_1 < 2{\cdot}5$ degrees (see Fig. 8). This implied that the dynamic stiffness of the system increased as the amplitude of the motion decreased. The increase was probably due to the variations in structural friction and internal damping of the wing. Hence, for the measurement of the torsional derivatives at a particular frequency, the forcing amplitude θ_0 was made to be such that θ_1 was within the range $2{\cdot}5$ degrees $< \theta < 5{\cdot}0$ degrees.

The torsional damping derivative, which includes any structural damping that may be present, was obtained directly from (3), and is plotted in the form $\lambda_0 M_{\dot{\theta}}/\rho V l c_0^3$ against λ_0 in Fig. 11. The values given in Refs. 1 and 2 are included for comparison. In still air, the torsional damping increased with decreasing amplitude for $\theta_1 < 2{\cdot}5$ degrees; but for $2{\cdot}5$ degrees $< \theta_1 < 5{\cdot}0$ degrees, its value was approximately $M_{\dot{\theta}} = - 0{\cdot}03$ for all frequencies.

The torsional stiffness derivative was obtained from (4) by plotting $S(V, p)$ against p^2 and considering the differences between $S(V, p)$ and $S(o, p)$. It was found that $S(o, p)$ plotted linearly over the whole practical range of frequencies and that, for frequencies corresponding to $\lambda_0 > 1$, $S(V, p)$ also plotted linearly (see Fig. 10). This indicated that over the linear range, $m_\theta - M_\theta$ and $G_3 - M_{\ddot{\theta}}$ could be assumed to be independent of frequency, and that the difference $S(V, p) - S(o, p) \equiv - M_\theta + (M_{\ddot{\theta}} + I_E)p^2$ would be linear for any particular wind speed. The values of the difference, expressed as a non-dimensional coefficient, are given in Table 1. This coefficient is not the true aerodynamical derivative, as it includes the still air virtual inertia effect, but it is the appropriate derivative for calculations of flutter speed in which the torsional moment of inertia is assumed to be as determined experimentally in air. The corresponding virtual inertia term was estimated as in Ref. 6, and a value of $I_E/\rho l c_0^4 = 0{\cdot}00974$ was obtained; this is slightly less than the value for a flat plate of the same plan form as the thickness of the wing has been taken into account. The value of the true derivative was then deduced and is listed in Table 1 for comparison with the result obtained theoretically in Ref. 2, with which it is in good agreement. The value deduced by the use of the fundamental derivatives $l_a = 1{\cdot}6$, $m_a = - 0{\cdot}4$ given in Ref. 1 was $- 0{\cdot}0329$ as compared with the mean experimental value of $- 0{\cdot}0453 - 0{\cdot}0066\lambda_0^2$. A value of $- 0{\cdot}0408$ is obtained if the aerodynamic centre is taken to be at $0{\cdot}238c$ as suggested in Ref. 4, and if m_a only is altered to give $- m_a/l_a = 0{\cdot}238$.

It was also noted that the dynamic torsional stiffness, $m_\theta = 10$, given by the intercept of the line $S(o, p)$ on the axes $p = 0$, was greater than the static value of $9{\cdot}78$ lb. ft./rad. for the stiffness of the whole system. The static stiffness of the wing alone was $2{\cdot}87$ and the difference of $0{\cdot}22$ between the static and dynamic stiffnesses of the system was probably due to a change of this amount in the stiffness of the wing structure. This represents an increase of $7{\cdot}7$ per cent. as compared with an increase of $11{\cdot}6$ per cent. obtained in the tests on a wooden spar described in Appendix IV of Ref. 5.

§6. *Static Aerodynamical Torsional Stiffness.*—Measurements of $m_\theta - M_\theta$ for various wind speeds were also made corresponding to a non-oscillatory condition of the wing. In these tests the twists at the reference section corresponding to a series of known applied twisting moments were measured, and the required derivative was deduced by plotting the results. To increase accuracy, the torsional stiffness m_θ was made about twice the value of M_θ for a particular wind speed. The values of M_θ, shown plotted against V^2 in Fig. 12, give a value of $0{\cdot}0620$ for the coefficient $M_\theta/\rho V^2 l c_0^2$ as compared with the value $0{\cdot}0644$ deduced by strip theory in Ref. 2.

This is considerably higher than the experimental value obtained for the dynamic torsional stiffness derivative (see Table 1). From these results, it is evident that the derivative applicable to oscillatory motion must not be used to predict divergence speed. The divergence speeds corresponding to various values of m_θ were predicted and found to be in good agreement with the experimental results (see Table 2b).

§7. *Divergence Speed Tests.*—The wing was made infinitely stiff in flexure and set in its zero pitching moment position. The torsional elastic stiffness m_θ for this series of tests was 2·87 lb. ft./rad. As the divergence condition of the wing was not very definite, observations were made at various wind speeds in the critical range (see Table 2a). The values of the divergence speeds corresponding to $m_\theta = 2{\cdot}52$ and $10{\cdot}45$ are also given for comparison in Table 2b.

§8. *Critical Flutter Speed Tests.*—In preliminary tests with $m_\theta = 2{\cdot}52$, flutter occurred at very low wind speeds. In order to obtain higher critical speeds, the torsional stiffness of the wing was increased from $m_\theta = 2{\cdot}52$ to $10{\cdot}45$ by cross-connecting the spars at the root. This resulted in a slight alteration of the torsional mode, which however did not sensibly influence the values of the inertial constants. The flexural stiffness was varied to give values ranging from 0 to $17{\cdot}5$ for the stiffness ratio parameter r. For each value of r, three critical speeds were observed corresponding to :

(i) spontaneous flutter,

(ii) flutter started by an initial twist of 2·5 degrees at the reference section,

(iii) maintained oscillations of 2·5 degrees amplitude started artificially.

The critical speed for (i) depended on the disturbances in the airstream ; the greater the disturbance the lower the critical speed. As a sudden change in wind speed for a low value of r would induce a greater flexural displacement than an equal change at a high value of r, the corresponding critical speeds are not strictly compatible. The wing oscillations for this critical condition increased slowly in amplitude up to about 2·5 degrees and then increased very rapidly. The variation in the rate of increase was due to the decrease in the hysteresis damping and in the effective stiffness of the wing with increasing amplitude (see §5). Hence, the spontaneous critical speeds in these tests do not correspond to the predicted speeds in the calculation of which the effect of internal friction has been neglected. For (ii), the wing was given an initial twist of approximately 2·5 degrees for each test. This gave rise to small oscillations which grew rapidly at the critical speed. For (iii), the wing was artificially disturbed to give initial oscillations of about 2·5 degrees amplitude in twist, and the wind speed at which these were maintained was observed. The frequency of the maintained oscillation was measured by means of a chronograph. The various critical speeds and frequencies for Wing Condition II are plotted against r in non-dimensional form in Figs. 13 and 14. Some results for Wing Condition I and $m_\theta = 2{\cdot}52$ are given in Fig. 15.

The differences between the highest and the lowest critical speeds observed when $m_\theta = 10{\cdot}45$ were not as great as for the tests when $m_\theta = 2{\cdot}52$ (see Fig. 13). This is probably due to the increased influence of the torsional stiffness in relation to the frictional and damping effects of the internal structure. Any further increase in the torsional stiffness would tend to make the spontaneous flutter speeds identical with the critical speeds for maintained oscillations of 2·5 degrees amplitude.

§9. *Calculation of Flutter Speeds and Frequencies.*—In the calculation of critical speeds for flutter and the corresponding frequencies, the derivative values deduced from R. & M. 1782 were used (see Table 4). The calculations were repeated with $k_3 = -0{\cdot}0453 + 0{\cdot}00315\lambda_0^2$, which was the value determined experimentally. The experimentally obtained inertial constants were used in both cases. The predicted critical speeds, frequency parameter values, and flutter frequencies, are plotted against r in Figs. 13 and 14. Some theoretical curves given in Ref. 2 are included for comparison. The derivatives used in Ref. 2 were deduced from two-dimensional theory and their approximate values for $1{\cdot}6 < \lambda_0 < 5{\cdot}0$ are given in Table 4 as a matter of interest.

The predicted flutter frequencies agreed well with experiment in all cases, but the experimental critical speeds and λ_0 values were not in such good agreement (see Fig. 13).

Some calculations of $Vc\sqrt{\rho}/\sqrt{m_0/dc_m^2}$ were also made with the inertial constants for Wing Condition II corrected for virtual inertia effects. Values of 5·12, 13·6, and 36·5 were obtained for $r = 0$, 3, and 4 respectively by the use of the derivatives deduced from Ref. 1. These results are much higher than the experimental values, probably due to the assumption that c_1 and c_3 are zero.

The corresponding results using the corrected inertia values and the derivatives given in Ref. 2 are being calculated by Frazer and Skan, and will be described in detail in another note.

§10. *Effect of Wing Tip Shape on Flutter.*—Tests were carried out by the addition to the wing of tip sections of equal area and having practically the same inertia values. Two cases were investigated :—

(1) Square cut tip section of span 4·77 in. and the same taper ratio as the original wing (see Fig. 16).

(2) Rounded tip section of span 6 in. (see Fig. 17).

The inertia values of the modified wing referred to the reference section at 0·7 span of the original wing are given for each case in Table 5.

In the flutter tests, the torsional stiffness of the wing $m_\theta = 10·45$ lb.ft./rad., was kept constant and the flexural stiffness l_ϕ was varied as before. The corresponding lowest critical speeds at which maintained oscillations could be produced by artificial disturbances, and the spontaneous critical speeds for flutter were observed (see Table 6).

The results show no appreciable differences due to the shape of wing tip used.

§11. *Conclusions.*—The experimental results indicate that the direct flexural and torsional dampings can be estimated with fair accuracy from the fundamental derivative values given in R. & M. 1782, but the static and dynamic torsional stiffness derivatives are given more accurately by strip-theory as in Ref. 2.

The estimated critical speeds obtained by using the experimentally determined inertias and the derivative values of R. & M. 1782 are too high and the corresponding frequency parameters too low ; better agreement is obtained by using the measured instead of the estimated value of k_3 (see §5). The predicted speeds obtained by using the true inertial constants instead of the inertia values given by resonance experiments in air are much too high. It appears therefore that the experimentally determined inertial coefficients must be used with the derivatives of R. & M. 1782 to predict critical speeds with any accuracy.

REFERENCES

No.	*Author*	*Title, etc.*
1	W. J. Duncan and H. M. Lyon	Calculated Flexural-Torsional Flutter Characteristics of Some Typical Cantilever Wings. R. & M. 1782, 1937.
2	R. A. Frazer	Flexure-Torsion Flutter Derivatives for Semi-Rigid Wings. R. & M. 1942, 1945.
3	W. P. Jones	The Virtual Inertias of a Tapered Wing in Still Air. R. & M. 1946, 1945.
4	G. A. Naylor	Some Theoretical Comments on Recent Results of the N.P.L. Model Tests on Wing Flutter. 5047—0·208. R.A.E. Report A.D.3163. (Unpublished.)
5	R. A. Frazer and W. J. Duncan	The Flutter of Aeroplane Wings. R. & M. 1155, 1928.
6	L. Bairstow	Applied Aerodynamics.
7	E. N. Jacobs and W. C. Clay	Characteristics of the N.A.C.A.23012 Airfoil from Tests in the Full-Scale and Variable-Density Tunnels. N.A.C.A. Report No. 530.

TABLE 1

Torsional Stiffness Derivative

V (ft./sec.)	$\frac{-M_\theta}{\rho V^2 l c_0^2} + \frac{\lambda_0^2(M_{\ddot{\theta}} + I_E)}{\rho l c_0^4}$	$\frac{-M_\theta}{\rho V^2 l c_0^2} + \frac{\lambda_0^2 M_{\ddot{\theta}}}{\rho l c_0^4}$	
		Corrected for Virtual Inertia	From Ref. 2
30·2	$0{\cdot}00278\lambda_0^2 - 0{\cdot}0452$	$-0{\cdot}00696\lambda_0^2 - 0{\cdot}0452$	$-0{\cdot}00948\lambda_0^2 - 0{\cdot}0446$
40·2	$0{\cdot}00302\lambda_0^2 - 0{\cdot}0459$	$-0{\cdot}00672\lambda_0^2 - 0{\cdot}0459$	$-0{\cdot}00948\lambda_0^2 - 0{\cdot}0446$
50·3	$0{\cdot}00365\lambda_0^2 - 0{\cdot}0449$	$-0{\cdot}00609\lambda_0^2 - 0{\cdot}0449$	$-0{\cdot}00948\lambda_0^2 - 0{\cdot}0446$
Mean Value ..	$0{\cdot}00315\lambda_0^2 - 0{\cdot}0453$	$-0{\cdot}00659\lambda_0^2 - 0{\cdot}0453$	$-0{\cdot}00948\lambda_0^2 - 0{\cdot}0446$

TABLE 2a

Divergence Tests

Test No.	m_θ (lb. ft./rad.)	V (ft./sec.)	Range of Twist	Remarks
1	2·87	34·2		Wing returned to position of slight *—ve* twist from deflections either side of zero.
2	2·87	35·8	0° . . . —2·0°	Neutral equilibrium between these limits.
3	2·87	37·0	1·5° . . . —4·0°	Neutral equilibrium between these limits.
4	2·87	38·1	3° . . . —6·0°	Neutral equilibrium over range but tendency to creep from 0° to —6·0°.
5	2·87	40·4	5° . . . —7·0°	Unstable over range.

TABLE 2b

m_θ (lb. ft./rad.)	Divergence Speed (ft./sec.)			$V_d\sqrt{\rho}/\sqrt{m_\theta/dc_m^2}$		
	Experimental	Estimated from §6	Estimated from Ref. 2	Experimental	Estimated from §6	Estimated from Ref. 2
2·52	37·2	36·4	35·7	3·55	3·47	3·40
2·87	38·1	38·8	38·1	3·40	3·47	3·40
10·45	73·4	74·1	72·6	3·44	3·47	3·40

TABLE 3

Inertia Values

Inertial Coefficients	Experimental		Estimated Virtual Inertias	Corrected Values	
	I	II		I	II
$A_1/\rho l^3 c_0^2 \equiv a_1$	1·873	1·618	0·322	1·551	1·296
$G_3/\rho l c_0^4 \equiv g_3$	0·0701	0·0606	0·0097	0·0604	0·0509
$P/\rho l^2 c_0^3 \equiv a_3$	0·123	0·110	0·042	0·081	0·068

TABLE 4

Theoretical Derivatives

Derivative	Ref. 3	Ref. 1
$c_1 \quad (\equiv \bar{L}_1)$	$0{\cdot}4113 - 0{\cdot}3013\lambda_0^2$	0
$b_1\lambda_0 \ (\equiv \bar{L}_2)$	$0{\cdot}3341 + 0{\cdot}9543\lambda_0$	$0{\cdot}937\lambda_0$
$k_1 \quad (\equiv \bar{L}_3)$	$1{\cdot}2853 - 0{\cdot}04433\lambda_0^2$	1·010
$j_1\lambda_0 \ (\equiv \bar{L}_4)$	$-0{\cdot}3348 + 0{\cdot}6790\lambda_0$	$0{\cdot}387\lambda_0$
$c_3 \quad (\equiv \bar{M}_1)$	$-0{\cdot}00642 - 0{\cdot}0444\lambda_0^2$	0
$b_3\lambda_0 \ (\equiv \bar{M}_2)$	$-0{\cdot}00879 - 0{\cdot}03219\lambda_0$	$-0{\cdot}0306\lambda_0$
$k_3 \quad (\equiv \bar{M}_3)$	$-0{\cdot}04464 - 0{\cdot}00948\lambda_0^2$	−0·0329
$j_3\lambda_0 \ (\equiv \bar{M}_4)$	$0{\cdot}0105 + 0{\cdot}0825\lambda_0$	$0{\cdot}0806\lambda_0$

TABLE 5

Inertia Values for Wing with Wing Tips

Inertial Coefficient	Wing with Square Cut Tip	Wing with Rounded Tip
$A_1/\rho l^3 c_0^2 \equiv a_1$	1·798	1·791
$G_3/\rho l c_0^4 \equiv g_3$	0·0672	0·0668
$P/\rho l^2 c_0^3 \equiv a_3$	0·117	0·117

TABLE 6

Critical Speeds (ft./sec.)

l_ϕ (lb. ft./rad.)	Wing with Square Cut Tip		Wing with Rounded Tip	
	Maintained Flutter	Spontaneous Flutter	Maintained Flutter	Spontaneous Flutter
163·7	38·3	43·0	36·9	42·2
355·8	30·6	37·8	29·0	36·4
625·3	24·1	34·8	23·2	34·7
953·2	25·8	35·9	25·6	35·9

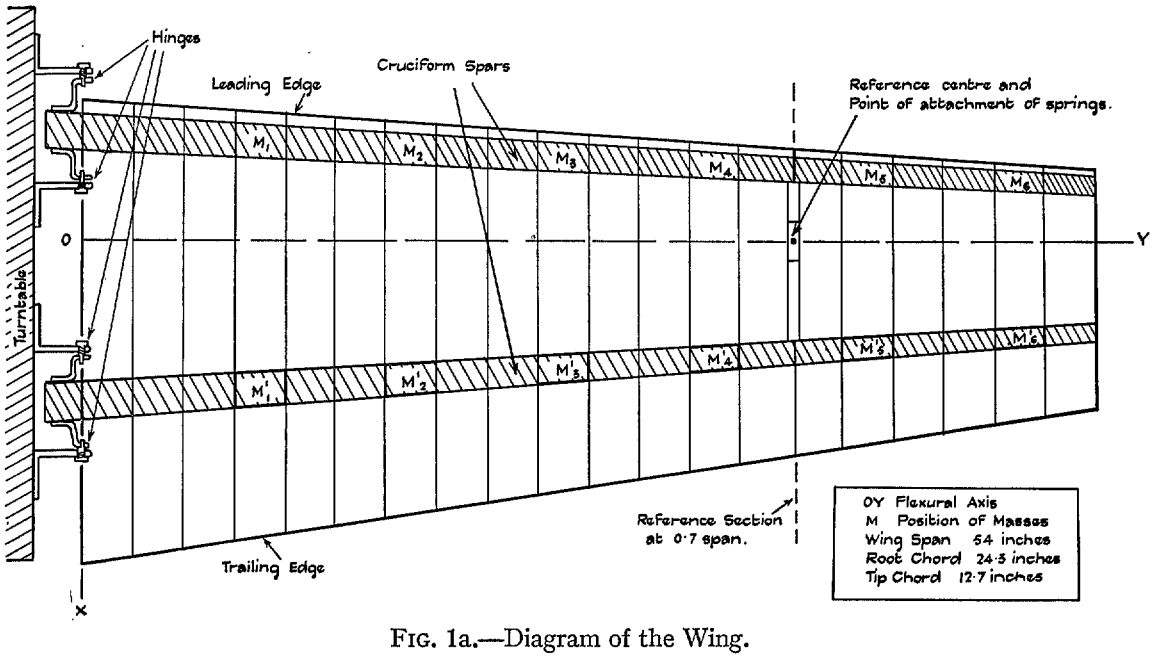

FIG. 1a.—Diagram of the Wing.

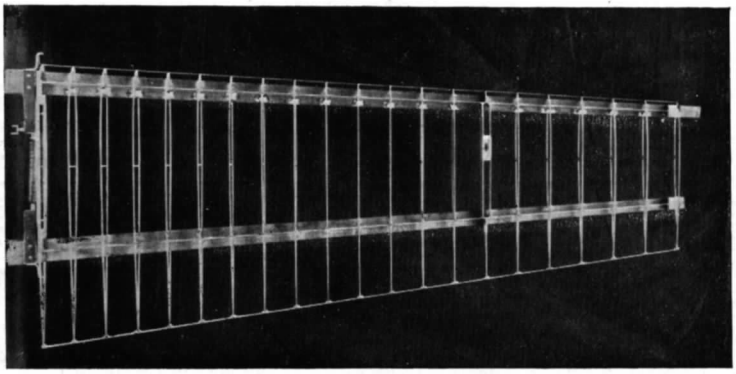

FIG. 1b.

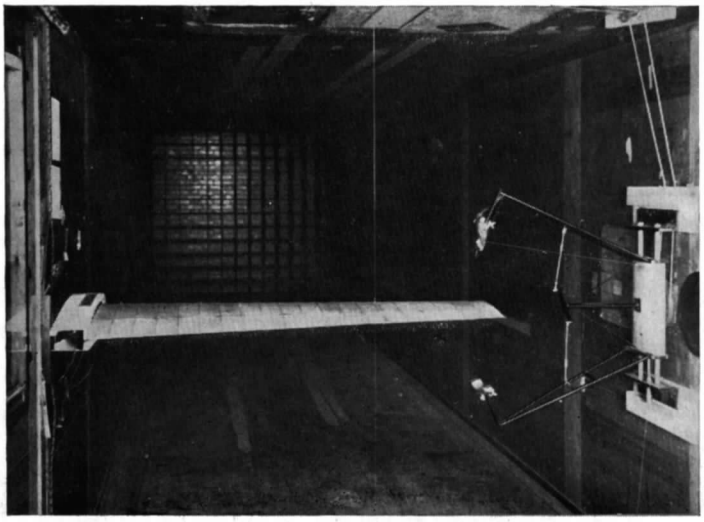

FIG. 2.

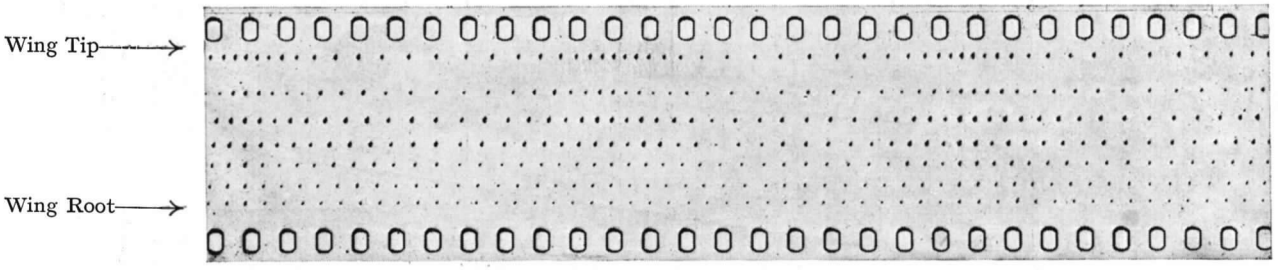

FIG. 3.

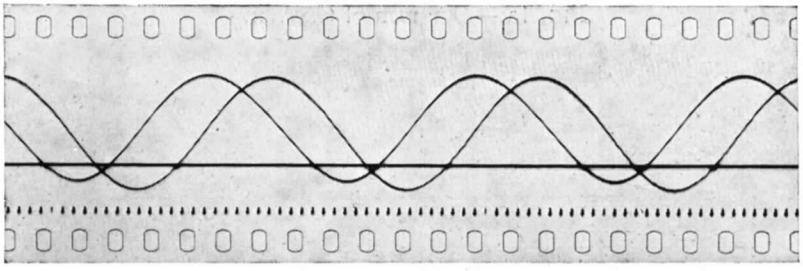

FIG. 4.

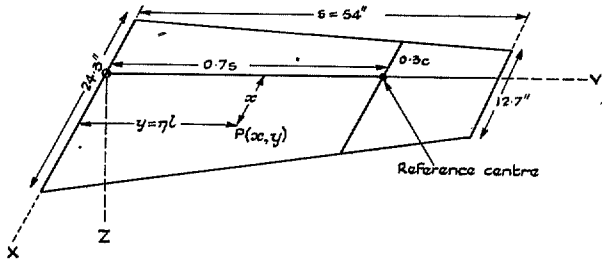

FIG. 5.—Wing Dimensions.

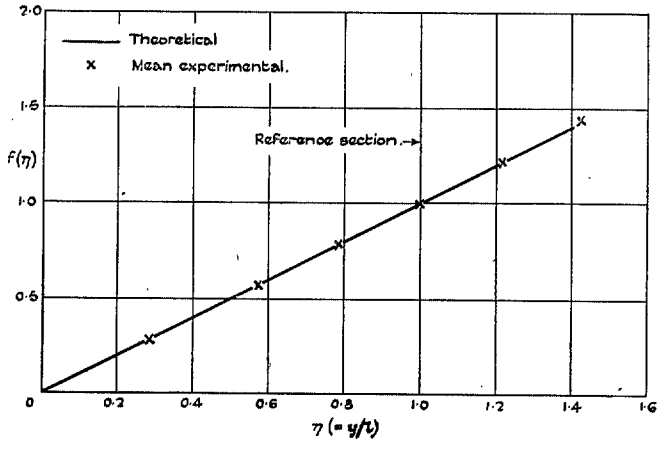

FIG. 6.—Flexural Mode.

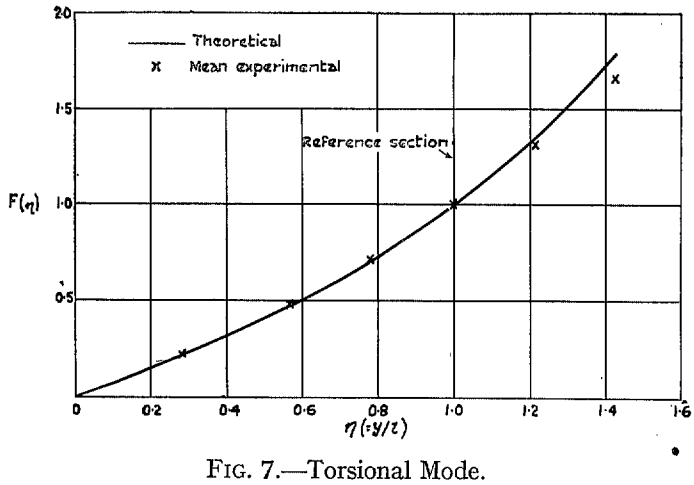

FIG. 7.—Torsional Mode.

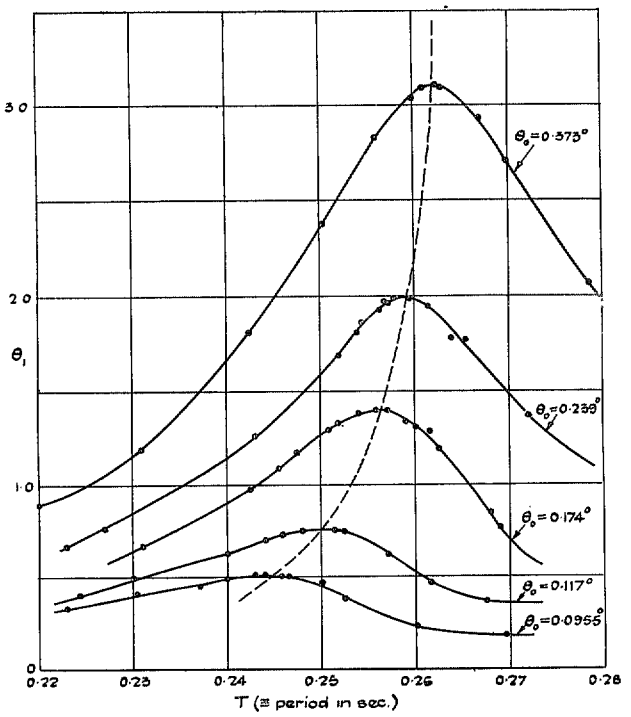

FIG. 8.—Variation of Resonance Frequency with Forcing Amplitude.

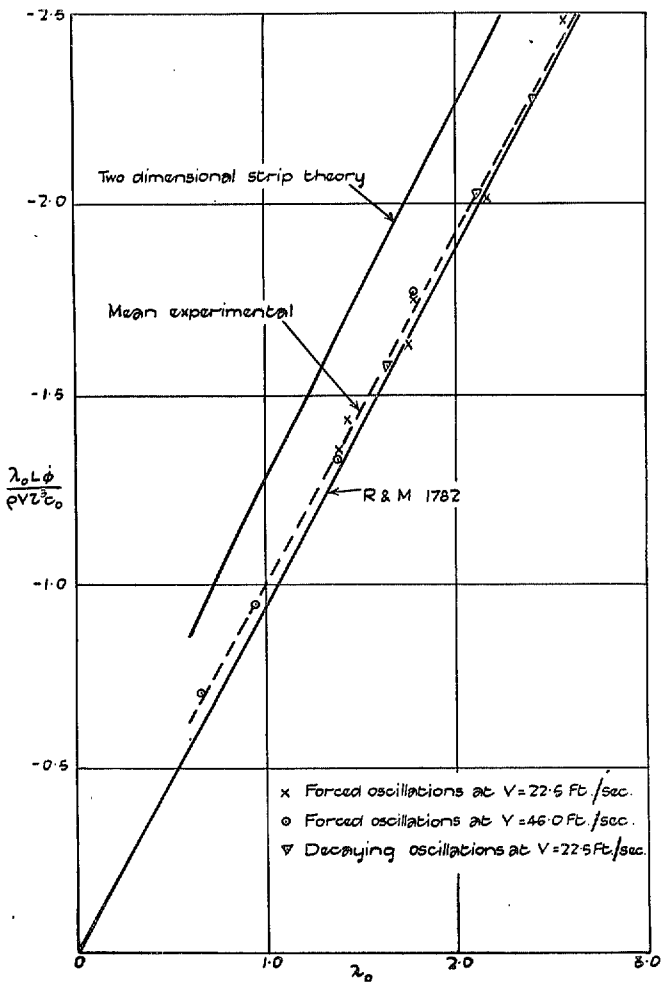

FIG. 9.—Aerodynamic Flexural Damping.

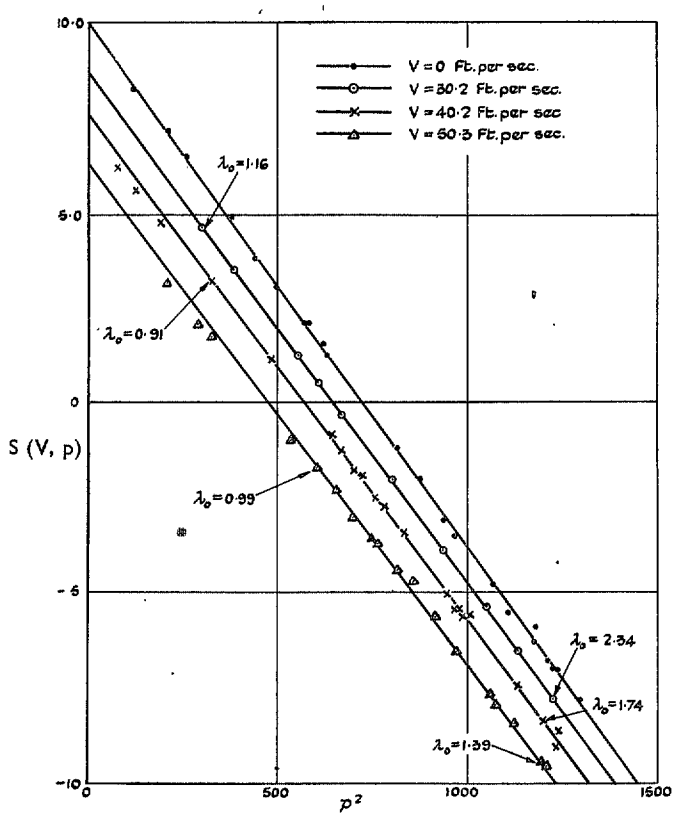

FIG. 10.—Variation of S (V, p) with Frequency at various Wind-Speeds.

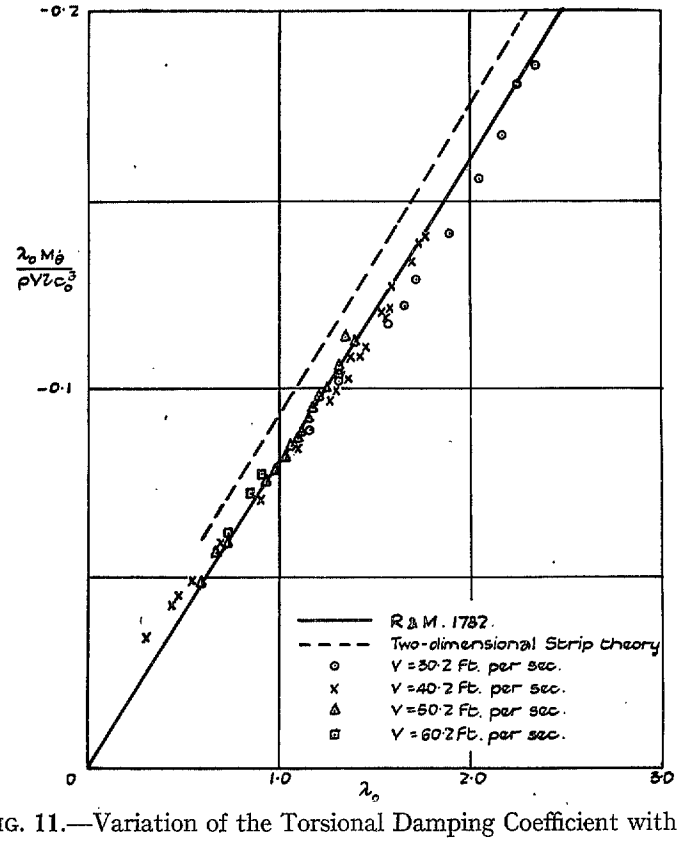

FIG. 11.—Variation of the Torsional Damping Coefficient with λ_0.

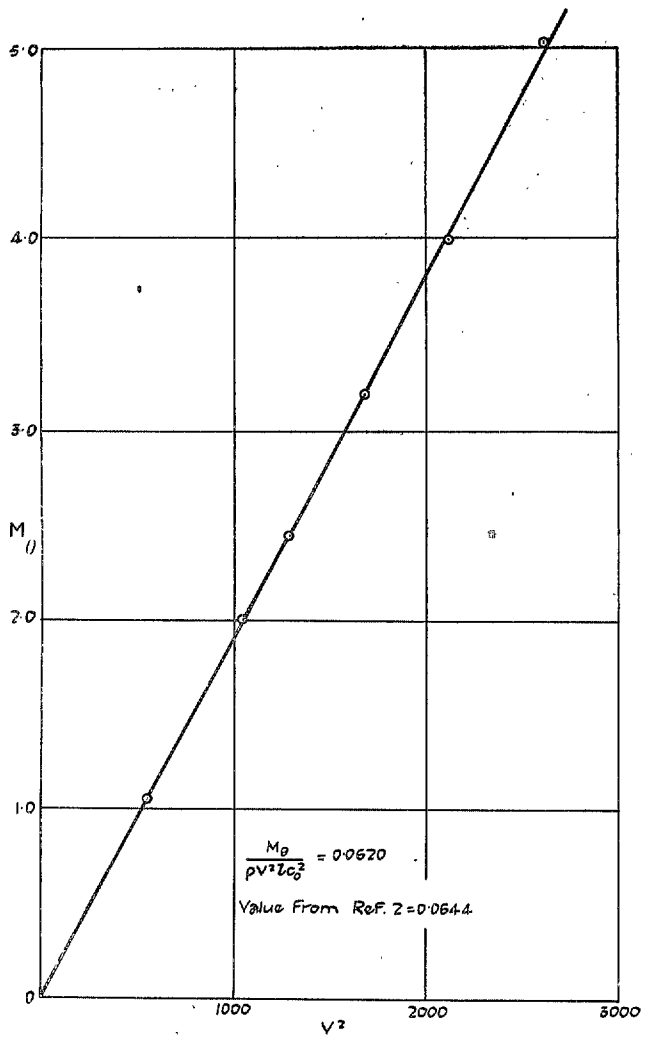

FIG. 12.—Static Aerodynamic Torsional Stiffness.

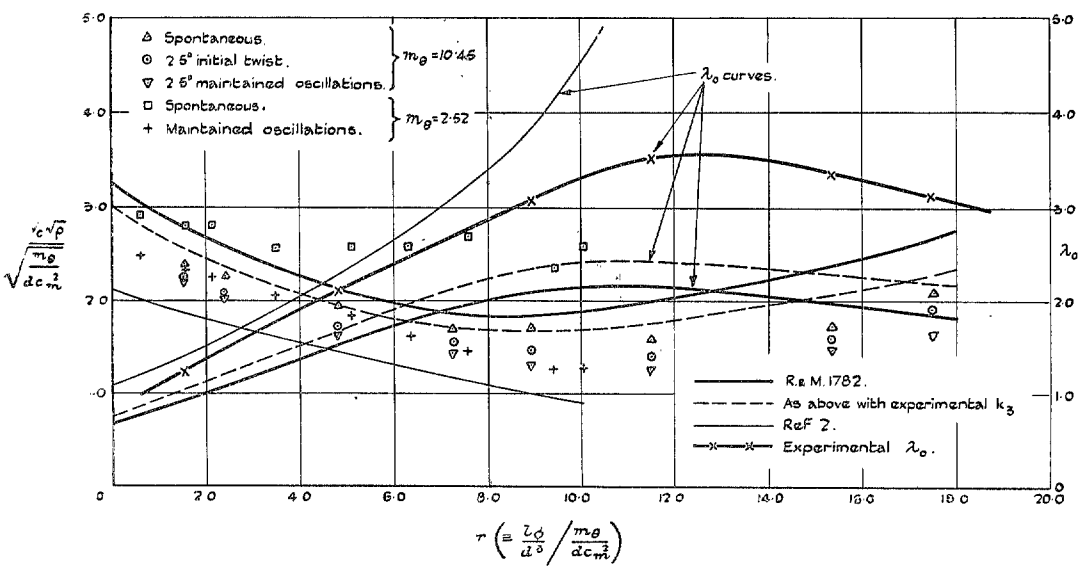

FIG. 13.—Critical Flutter Speed and Frequency Parameters.
(Wing Condition II.)

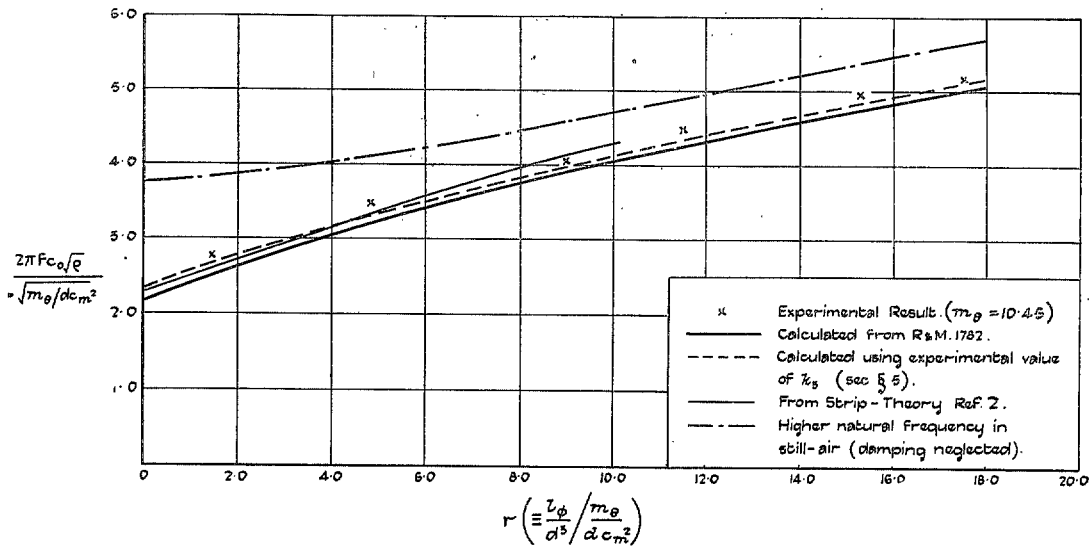

FIG. 14.—Frequency of Flutter at the Critical Speed.
(Wing Condition II.)

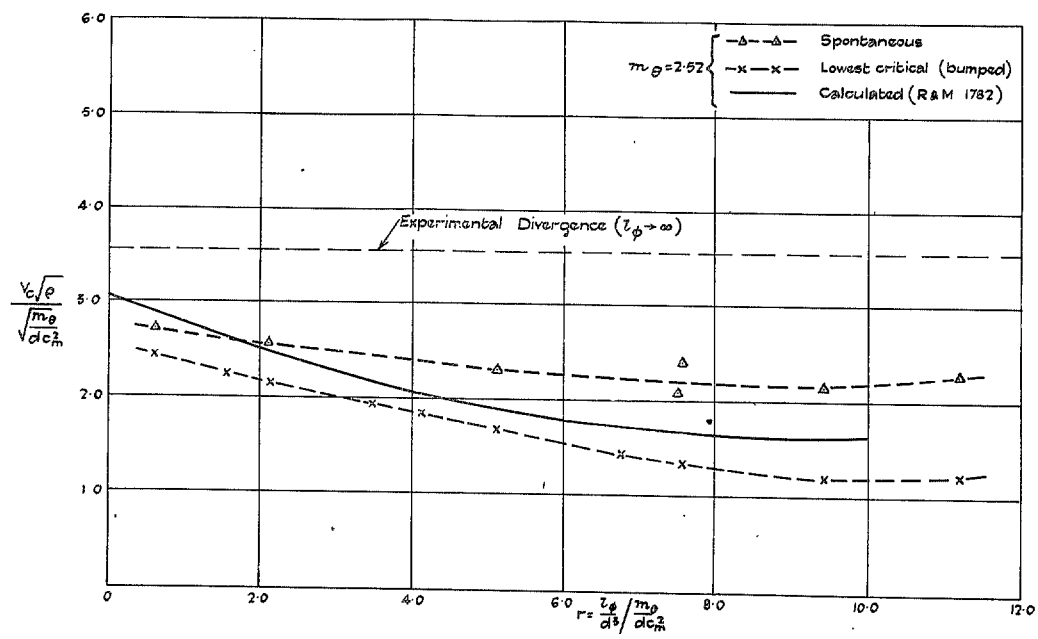

FIG. 15.—Critical Speeds for Wing Condition I.

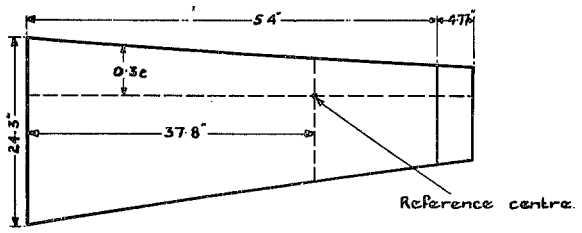

FIG. 16.—Wing with Square Cut Tip.

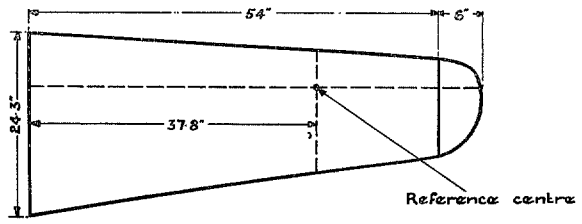

FIG. 17.—Wing with Rounded Tip.

(70676) Wt. 8/7116 9/45 Hw. G.377/1

Publications of the Aeronautical Research Committee

TECHNICAL REPORTS OF THE AERONAUTICAL RESEARCH COMMITTEE—

1934-35 Vol. I. Aerodynamics. £2.
Vol. II. Seaplanes, Structures, Engines, Materials, etc. £2.

1935-36 Vol. I. Aerodynamics. £1 10*s.*
Vol. II. Structures, Flutter, Engines, Seaplanes, etc. £1 10*s.*

1936 Vol. I. Aerodynamics General, Performance, Airscrews, Flutter and Spinning. £2.
Vol. II. Stability and Control, Structures, Seaplanes, Engines, etc. £2 10*s.*

1937 Vol. I. Aerodynamics General, Performance, Airscrews, Flutter and Spinning. £2.
Vol. II. Stability and Control, Structures, Seaplanes, Engines, etc. £3.

ANNUAL REPORTS OF THE AERONAUTICAL RESEARCH COMMITTEE—

1933-34 1*s.* 6*d.*
1934-35 1*s.* 6*d.*
April 1, 1935 to December 31, 1936. 4*s.*
1937 2*s.*
1938 1*s.* 6*d.*

INDEX TO THE TECHNICAL REPORTS OF THE ADVISORY COMMITTEE ON AERONAUTICS—

1909-1919 Reports and Memoranda No. 1600. 8*s.*

Prices are net and postage extra.

Obtainable from

His Majesty's Stationery Office

London W.C.2: York House, Kingsway
Edinburgh 2: 13A Castle Street
Manchester 2: 39-41 King Street
Cardiff: 1 St. Andrew's Crescent
Belfast: 80 Chichester Street
or through any bookseller.

S.O. Code No. 23-1945